BEHAVIOR OF SPENT FUEL ENTRAINED IN VOLCANIC MAGMA

B. Ross
Disposal Safety Inc.
1001 Connecticut Ave. NW, Suite 525 Washington, DC 20036

S. T. Smith
Howard University Washington, DC 20059

ABSTRACT

To date, performance assessments of the consequences of a volcanic eruption at Yucca Mountain have assumed that all fuel that comes into contact with erupting magma disintegrates as a result of physical abrasion and forms particles of respirable size that are entrained within larger droplets of magma which erupt into the air. It has been assumed that the spent fuel remains a distinct solid phase at all times, but this assumption requires re-examination. Uranium oxides do not melt at the temperatures of basaltic magmas, but the solubility of UO_2 in basaltic magma is approximately 20% by weight. For small particles, the rate-limiting process in dissolution will likely be diffusive mass transfer away from the surface of the solid particle. We calculated the dissolution time of the largest respirable particle, with diameter of 10 μm, for a range of reasonable diffusion constants and obtained a value between 2.1 sec and 21 sec. Consequently, small respirable particles of spent fuel that are formed when magma intrudes into a repository can be expected to dissolve into the magma before reaching the surface. Because dissolution time varies with the square of the particle radius, 1-mm particles will have a dissolution time of 6 hours to 2 days, and larger particles will dissolve even more slowly. Thus, respirable particles of spent fuel will dissolve into the magma, but larger pieces of fuel will remain solid. The net effect is that respirable ash particles will be formed entirely by solidification of small droplets of magma and will be depleted in refractory spent fuel components compared to the average composition of the erupted material.

INTRODUCTION

When the safety of the proposed HLW repository at Yucca Mountain, Nevada, is analyzed, one of the major exposure pathways that must be considered is dispersal of spent fuel in the atmosphere during a volcanic eruption. In analyses of this pathway, the largest contribution to dose during the first 2000 years after emplacement is due to inhalation of resuspended radioactive particles.[11] Only that portion of the radioactive inventory which is dispersed into the atmosphere as particles of respirable size (less than 10 μm diameter) contributes to such doses.

To date, performance assessments have assumed that all fuel that comes into contact with erupting magma disintegrates as a result of physical abrasion and forms solid particles which are, when loose, of respirable size. This assumption is based on experimental studies of the grinding of oxidized spent fuel [8]. (Note that experimental grinding of unoxidized UO_2 produces particles with an average diameter of 20 μm, which is larger than respirable size.)

The performance assessments assume that all of the abraded fuel particles are entrained within larger droplets of magma which erupt into the air. During this process, the spent fuel is assumed to remain a

distinct solid phase at all times. However, assumptions about the size distribution of the ash droplets have varied:

- In the ASHPLUME model, which both DOE and NRC have used to calculate how far the ash particles travel, a probabilistic formula is used to compute the amount of spent fuel incorporated within ash particles of any given size.

- In calculations of human inhalation and ingestion rates, the TSPA-SR [11] assumes that one-third of the spent fuel is contained in particles of less than 10 μm diameter and the remaining two-thirds is contained in particles of between 10 and 100 μm diameter.

Performance assessments can be improved by considering interactions between liquid magma and spent fuel while they are in contact. Such contact is to be expected because the large mass and thermal inertia of waste packages will prevent rapid disintegration of waste containers that may come into contact with hot gases during the initial moments of a volcanic eruption. Container failures can be expected only after contact with liquid magma, which would have a much greater volumetric heat capacity and a much longer residence time in repository drifts than the erupting gases.

The melting points of uranium oxides are far above the 1200 °C temperatures of typical basaltic magmas. However, the solubility of UO_2 in basaltic magma has been measured as approximately 20% by weight [13]. This implies that a 10-μm-diameter spherical particle of UO_2 coated by a 7.9-μm-thick shell of magma can completely dissolve in the magma. (The computation assumes that the UO_2 particle is 4 times denser than the saturated solution of UO_2 in magma.)

How much time does it take for such a particle to dissolve after it comes into contact with the magma? Most likely, the rate-limiting process will be mass transfer away from the surface of the solid particle. The distance scale is sufficiently small that diffusion is likely to be the dominant mass transfer mechanism.

MATHEMATICAL FORMULATION

The dissolution of a solid sphere is a well-known mathematical problem for which no exact analytical solution is available. The governing equation is

$$\frac{1}{D}\frac{\partial C}{\partial t} = \frac{2}{r}\frac{\partial C}{\partial r} + \frac{\partial^2 C}{\partial r^2} \qquad \text{(Eq. 1)}$$

with initial and boundary conditions

$$C(r,0) = 0$$

$$C[(a(t),t] = S$$

$$C(r,t) \to 0 \quad \text{as} \quad r \to \infty$$

and the location $a(t)$ of the moving boundary is given by the Stefan condition

$$\frac{da}{dt} = \frac{D}{\rho - S}\left(\frac{\partial C}{\partial r}\right)_{r=a(t)} \qquad \text{(Eq. 2)}$$

with

$$a(0) = a_0.$$

In these equations, D is the diffusivity and S is the solubility of UO_2 in magma, a_0 is the initial radius of the solid particle, and ρ is the density of solid UO_2. Note that the same equations describe the melting of a solid sphere, whose temperature is initially at the melting point, surrounded by warmer liquid [2].

The moving boundary condition makes this problem very difficult to solve analytically. Carslaw and Jaeger [2], on p. 295, evaluate the growth of a solid sphere in a supercooled liquid (equivalent to precipitation from a supersaturated solution). But their result is approximate, to use it one must find the roots of a non-linear algebraic equation involving error functions and exponentials, and in any case the formula is not applicable to a solid melting in warmer liquid (equivalent to dissolution in an undersaturated liquid).

Rough estimates of melting or dissolution time are available. These can be expressed in terms of a characteristic time,

$$\tau = \frac{a_0^2}{2D}, \qquad \text{(Eq. 3)}$$

which is interpreted physically as the time after which the root-mean-square displacement of a diffusing particle is a_0 [9].

One such estimate is obtained by the "quasi-static approximation" which approximates the temperature (or solute concentration) in the liquid by the solution for a fixed boundary [5]. With this approximation, one finds that $a(t) = 0$ at

$$t = \frac{\tau(\rho - S)}{S}. \qquad \text{(Eq. 4)}$$

However, the quasi-static method is only accurate in the limit as $\eta \equiv S/(\rho - S) \to 0$, and therefore is not reliable for our problem where $\eta = 0.25$.

An alternative estimate, which is more physically based, is obtained by observing that a spherical solid particle of radius a_0 can be dissolved in a magma sphere of radius $a_0(\rho/S)^{1/3}$. The time required for the solute to mix into this volume of liquid is the time that a solute particle travels a root-mean-squared distance equal to the radius of the magma sphere, or

$$t = \tau(\rho/S)^{2/3}. \qquad \text{(Eq. 5)}$$

The approximate formulas (4) and (5) disagree and there is no clear reason for preferring either of them. A numerical solution of the governing equations is therefore very much to be desired.

The challenge to any numerical solution is resolving the moving boundary (2). Boundary conditions must be applied at a node or interface of a finite-difference or finite-element grid to be exact, and this is impossible with a moving boundary. If one tries to approximate the moving boundary, numerical errors are unavoidable and their magnitude is hard to quantify. For this reason, it is highly desirable to transform the governing equation in such a way that the boundary is stationary.

Numerical methods used for tracking arbitrarily shaped interfaces are classically categorized as either surface tracking (Lagrangian) methods or volume tracking (Eulerian) methods. In surface tracking methods the domain is discretized using a grid that continuously adapts to the shape of the interface. Grid

rearrangement and motion terms must be incorporated since in this case the grid becomes distorted and must be regenerated each time. This can also affect the accuracy of the solver. The volume tracking methods employ a fixed grid and hence the shape of the interface is not explicitly tracked but is reconstructed from the properties of appropriate field variables. The discretization process is simplified in this case, but when the interface is arbitrarily shaped, improved resolution in the regions where there are sharp gradients requires local iterative refinements [12]. Most recently, combined Lagrangian-Eulerian methods, employed frequently in fluid mechanics, have been applied to moving boundary problems.

For one-dimensional problems, an alternative to tracking the front is to fix the boundary with a transformation of coordinates. Crank [4] reviews several transformations and solution methods starting with Landau's[6] transformation and its solution by Crank[3]. In the present study the space coordinate is transformed using the substitution:

$$u = r - a(t), \tag{Eq. 6}$$

which yields the boundary condition

$$C(0,t) = S. \tag{Eq. 7}$$

The time derivatives of C in the two coordinate systems are related by

$$\begin{aligned}\frac{\partial C(r,t)}{\partial t} &= \frac{\partial C(u,t)}{\partial t} - \frac{\partial C(u,t)}{\partial u}\frac{du}{dt} \\ &= \frac{\partial C(u,t)}{\partial t} - \frac{\partial C(u,t)}{\partial u}\frac{da}{dt} \\ \frac{\partial C(r,t)}{\partial t} &= \frac{\partial C(u,t)}{\partial t} - \frac{D}{\rho - S}\frac{\partial C(u,t)}{\partial u}\left(\frac{\partial C(u',t)}{\partial u'}\right)_{u'=0}\end{aligned} \tag{Eq. 8}$$

Inserting (6) and (8) into (1) yields a pair of coupled equations in the transformed coordinates u and t that can be solved by finite differences:

$$\frac{1}{D}\frac{\partial C(u,t)}{\partial t} = \left[\frac{2}{u+a} + \frac{1}{\rho - S}\left(\frac{\partial C(u',t)}{\partial u'}\right)_{u'=0}\right]\frac{\partial C(u,t)}{\partial u} + \frac{\partial^2 C(u,t)}{\partial u^2} \tag{Eq. 9}$$

$$\frac{da(t)}{dt} = \frac{D}{\rho - S}\left(\frac{\partial C(u',t)}{\partial u'}\right)_{u'=0} \tag{Eq. 10}$$

The initial radius of the UO_2 sphere is a_0. Equations (7), (9) and (10) as well as the initial condition and boundary condition at $r \to \infty$ are nondimensionalized with the characteristic length scale a_0 and the characteristic time scale $\tau = a_0^2/2D$, which was previously defined in Eq. (3). The concentration is normalized by the solubility of UO_2, S. These substitutions yield the following dimensionless equations:

$$\frac{\partial C^{å}}{\partial t^{å}} = \left[\frac{1}{u^{å} + a^{å}} + \frac{\eta}{2}\left(\frac{\partial C^{å}}{\partial u^{å}}\right)_{u^{å}=0}\right]\frac{\partial C^{å}}{\partial u^{å}} + \frac{1}{2}\frac{\partial^2 C^{å}}{\partial u^{å\,2}} \tag{Eq. 11}$$

$$\frac{da^{å}}{dt^{å}} = \frac{\eta}{2}\left(\frac{\partial C^{å}}{\partial u^{å}}\right)_{u^{å}=0} \quad \text{(Eq. 12)}$$

$$C^{å}(u^{å},0) = 0 \quad \text{(Eq. 13)}$$

$$C^{å}(0,t^{å}) = 1 \quad \text{(Eq. 14)}$$

$$C^{å}(u^{å},t^{å}) \to 0 \text{ as } u^{å} \to \infty \quad \text{(Eq. 15)}$$

where again , $\eta \equiv S/(\rho\text{-}S)$. As in Crank [4] and Segal et al.[10], the diffusion coefficient is used to define the characteristic time scale and does not explicitly appear in the nondimensionalized equations.

The governing equations are solved using central differences in the transformed space dimension, u, and a forward difference in time. For the Stefan condition on the boundary, a second order backward difference scheme: $[-3C^{å}(i)+4C^{å}(i+1)-C^{å}(i+2)]/(2\Delta u^{å})$ is used to evaluate the concentration gradient at $u^{å}$=0. An iterative procedure is used to ensure that the solution has converged at each time step which is typically achieved in 2-3 iterations. In this initial study, a uniform grid was used, however the continuing work employs nonuniform grids and higher order differencing schemes. The results of the latter studies will be reported at another time.

RESULTS

As discussed above, the solubility of UO_2 in basaltic magma has been measured as 20% by weight. Let us adopt for the density ρ of UO_2 a value of 12 g/cm^3 and for the density of basaltic magma 2.526 g/cm^3. An ideal mixture of 5% by volume of UO_2 and 95% by volume of basalt contains 20% UO_2 by weight and has a density of 3 g/cm^3. The solubility S of UO_2 is thus 0.6 g/cm^3. Hence the value of $\eta \equiv S/(\rho\text{-}S)$ =0.25.

While D has not been measured directly, it can be inferred from the measured diffusion constants of several other cations dissolved in basaltic magma. Such data have been compiled by Brady [1]. Adjusting these measurements by the ratios between the aqueous diffusion constants of these cations and the aqueous diffusion constants of water [7], one finds that the diffusion constant of UO_2 in basaltic magma at 1200 $^\circ$C lies between 2×10^{-8} and 2×10^{-7} cm^2/s. These values can be inserted in the formulae (4) and (5) to obtain initial order-of-magnitude estimates of particle dissolution times. The largest respirable particle has a diameter of 10 μm. Substituting $a_0 = 5\times10^{-4}$ cm into (3) gives a range of characteristic times τ from 0.625 s to 6.25 s. As estimated by Eq. (4), the dissolution time of the largest respirable particle falls between 2.5 s and 25 s. As estimated by Eq. (5), it falls between 1.83 s and 18.3 s.

Because in a numerical analysis the grid cannot have infinite size, a preliminary sensitivity analysis was conducted to determine the size of the modeled problem domain for grids with total lengths ranging from $2.0\times a_0$ to $10.0\times a_0$. The aim was to to determine how large a domain was needed to accurately approximate $u \to \infty$. The location of the moving boundary as a function of time for several test-grids

demonstrated that the numerical method was not sensitive to the length of the domain beyond a distance of $4.0 \times a_0$. Hence the grid with outer boundary at $8.0 \times a_0$ was used for the remainder of the study.

The results of the numerical solution are presented in Figures 1-3. Figure 1 shows the dimensionless concentration $C^{å}$ versus dimensionless radial position for at several time steps during the calculation. Figure 2 shows the dimensional results for the case $D = 2 \times 10^{-7}$ cm^2/s The shifting location of the boundary is clearly captured using the simple transformation given in Equation (6).

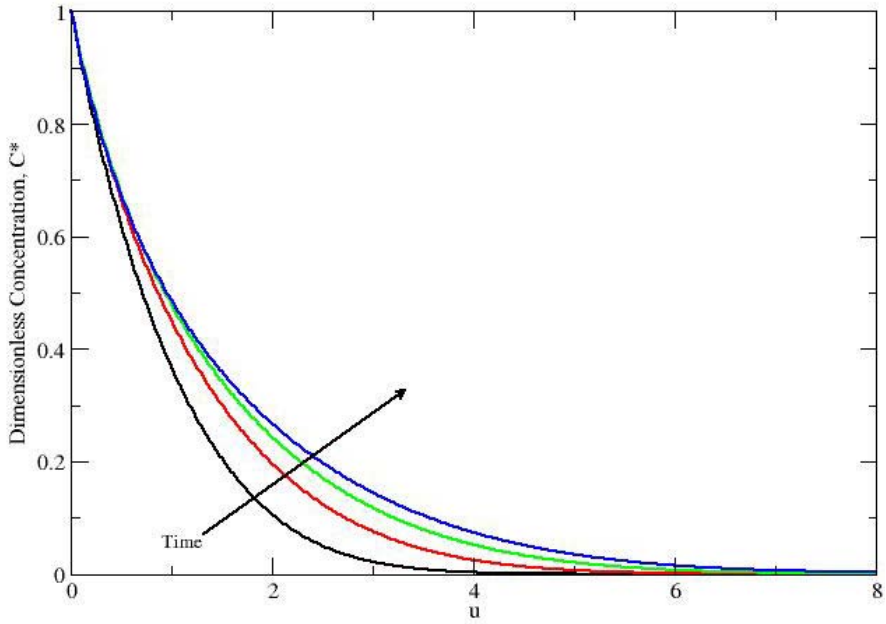

Fig. 1 Evolution of dimensionless concentration, D=2.0 x 10^{-7}

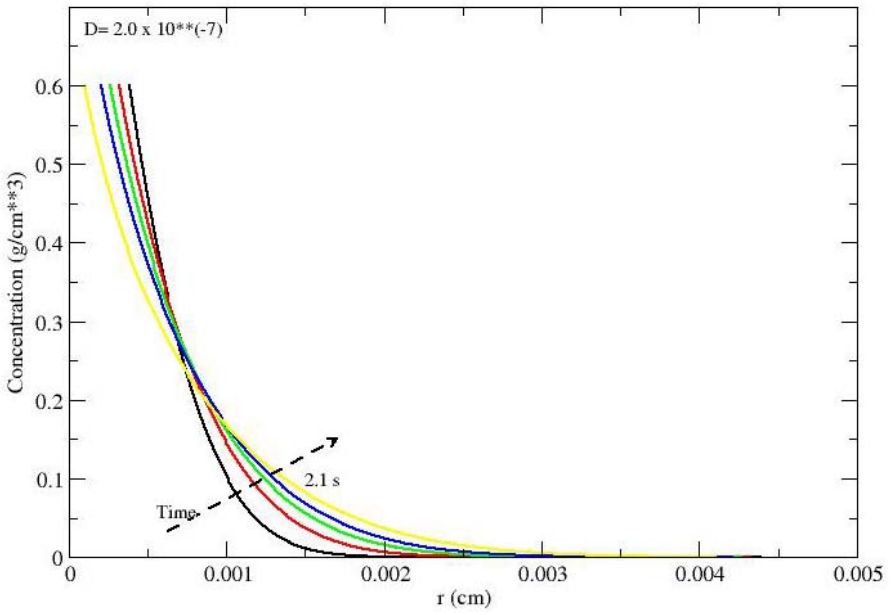

Fig. 2 Dimensional Concentration

The dissolution time in dimensionless coordinates was calculated to be $t^{\text{å}} = 3.289$. This yields a dissolution time for the $D = 2\times10^{-7}$ case of 2.1 seconds and for the $D = 2\times10^{-8}$ case 21 seconds. These times fall between the dissolution times predicted by the two rough approximations, Equations (4) and (5) as illustrated in Figure 3.

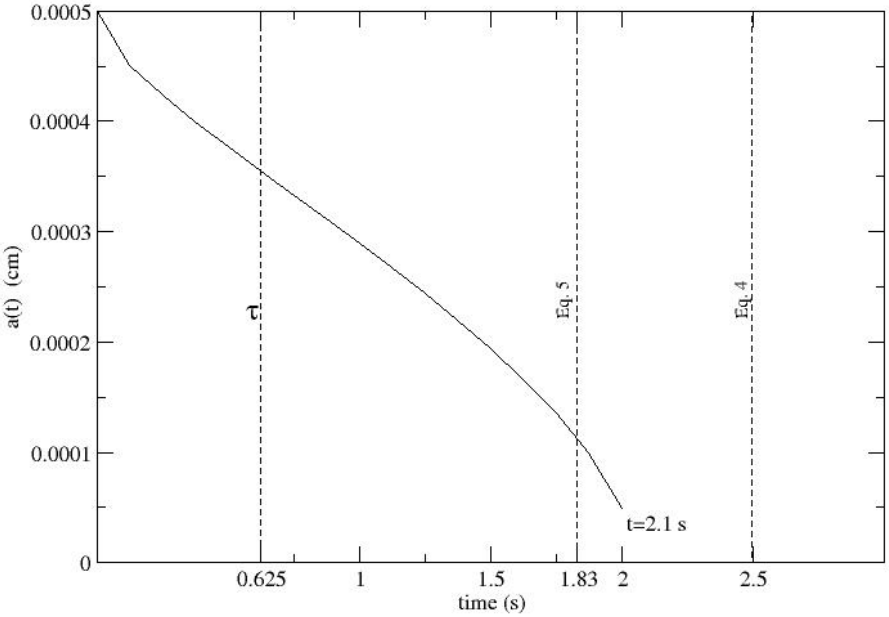

Fig 3 Dissolution Times

Validation of the numerical solution utilized the limiting behavior of equations (11) and (12) for $\eta = S/(\rho - S) << 2$. In this case, Eq. (12) shows that the rate of change of a(t) is small and the term multiplying η in Eq. (11) becomes negligible. This results in the steady state equation (Laplace's Equation) for the potential around a charged sphere whose solution is *C=a/r*. Applying the steady state solution in Eq. (12) gives $C'_{r=a} = -1/a$ so that the evolution of *a* behaves as $da/dt = -\eta/2a$. Integration of this equation gives $a^2/2 = -\eta t/2$ + const. so that the elapsed time from a=1 to a=0 is simply $1/\eta$. Figure 4 illustrates this limiting behavior for η=0.005. There is a short initial phase of rapid dissolution while the concentration profile relaxes from the initially infinite gradient at the particle surface to the *C=a/r* steady state. Thereafter, *da/dt* is indeed proportional to 1/a as indicated by the linear slope. The total dissolution time is *t** =207 which is very close to the expected limiting value of 1/ η =200.

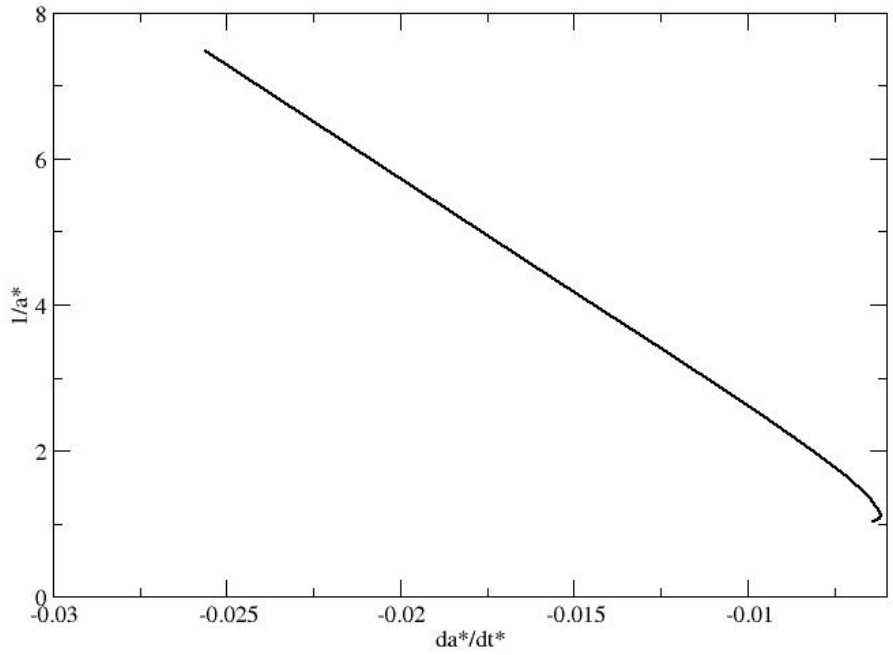

Fig. 4 Limiting behavior for $\eta = 0.005$

CONCLUSIONS

The calculated dissolution time of 2.1 s to 21 s implies that small respirable particles of spent fuel that are formed when magma intrudes into a repository can be expected to dissolve into the magma before the magma reaches the surface and erupts into the air. On the other hand, because of the a_0^2 dependence of the characteristic time (3) used to nondimensionalize the governing equations, dissolution times will increase with the square of the particle diameter. Thus the time required to dissolve a particle of 1 mm diameter will be between 5.8 hr and 58 hr, and larger particles will dissolve even more slowly.

The calculations show that respirable particles of spent fuel will dissolve into the magma, but larger pieces of fuel will remain solid. The net effect is that respirable ash particles will be formed entirely by solidification of small droplets of magma and will not contain solid inclusions of spent fuel. On the other hand, larger ash particles may contain undissolved pieces of spent fuel. Consequently, respirable ash particles will be depleted in refractory spent fuel components compared to the average composition of the erupted material.

REFERENCES

1 J. B. Brady, Diffusion data for silicate minerals, glasses, and liquids: in T. H. Ahrens, editor, *Mineral Physics and Crystallography: A Handbook of Physical Constants*, AGU Reference Shelf 2, American Geophysical Union, 1995, 269-290.

2 H. S. Carslaw and J. C. Jaeger, *Conduction of Heat in Solids*, 2nd ed., Clarendon, 1959, Chapter XI.

3 J. Crank, *Q. J. Mechanics and Applied Mathematics*, **10**, 220-231, 1957.

4 J. Crank, *Free and Moving Boundary Value Problems.* Oxford University Press, 1984.

5 M. E. Glicksman and A. Lupulescu, Diffusion in solids: Module 9, Spherical bodies, lecture notes,

2002. This document is available on the internet at www.rpi.edu/locker/40/001240/diff_mods/Diff09.ppt.

6 H.G. Landau, *Quarterly of Applied Mathematics*, **8**, 81-94, 1950.

7 D. R. Lide, *Handbook of Chemistry and Physics*, 75th ed., CRC Press, 1994, p. 5-90.

8 Miscellaneous Waste-Form FEPs, ANL-WIS-MD-000009, Civilian Radioactive Waste Management System Management & Operating Contractor, Attachment I (2000).

9 F. Reif, *Fundamentals of Statistical and Thermal Physics*, McGraw-Hill, 1965, p. 488.

10 Segal,G., K. Vuik, and F Vermolen. "A conserving Discretization for the Free Boundary in a Two-dimensional Stefan Problem." *J. Comp. Physics* **141**, 1-21, 1998.

11 "Total System Performance Assessment for the Site Recommendation," TDR-WIS-P-A-000001, Civilian Radioactive Waste Management System Management & Operating Contractor, pp. 3-206, 4-20 (2000).

12 W. Shyy, H. Udaykumar, M. Rao, and R. Smith. *Computational Fluids Dynamics with Moving Boundaries.* Taylor and Francis Pub., 1996.

13 H. R. Westrich, *J. Nucl. Mat.* **110**, 324-332 (1982).